Supplemental Materials

TXNIP suppresses the osteochondrogenic switch of VSMCs in atherosclerosis

Sang-Ho Woo[1, †], Dongsoo Kyung[2, †], Seung Hyun Lee[3], Kyu Seong Park[3], Minkyu Kim[3], Kibyeong Kim[3], Hyo-Jung Kwon[4], Young-Suk Won[5], Inpyo Choi[6], Young-Jun Park[7], Du-Min Go[1], Jeong-Seop Oh[1], Won Kee Yoon[5], Seung Sam Paik[8], Ji Hyeon Kim[8], Yong-Hwan Kim[9], Jae-Hoon Choi[3, ‡], Dae-Yong Kim[1, ‡]

Contents:

Methods

Mice

Txnip$^{-/-}$ (*Txnip* KO) and their littermate control *Txnip*$^{+/+}$ (WT) mice (C57BL6/J background) were obtained from the Korea Research Institute of Bioscience and Biotechnology.[55] For the bone marrow transplantation experiment, recipient C57BL6/J WT mice were obtained from the Central Lab. Animal, Inc. (Seoul, Korea). *Tagln*-cre mice (B6.Cg-Tg(Tagln-cre)1Her/J, strain no. 017491) and *Txnip*$^{flox/flox}$ mice (B6;129-*Txnip*^{tm1Rlee}/J, strain no. 016847) were obtained from the Jackson Laboratory (Bar harbor, ME, USA). To generate SMC-specific ablation of *Txnip* by Cre-mediated recombination under *Tagln* promotor, *Tagln*-Cre mice, and *Txnip*$^{flox/flox}$ mice were bred to give *Tagln*-Cre; *Txnip*$^{flox/flox}$ mice (SMC^{KO}). Their littermates that did not have *Tagln*-Cre were used as the control group (SMC^{WT}). For primary VSMC culture experiments, three to five week old C57BL6/J WT mice were used. Mice were housed at 22-24 °C with a standard light-dark cycle (12:12) and chow diet, and were freely accessible to diet and water. Atherosclerosis was induced by a single injection of adeno-associated virus serotype 8 (AAV8) encoding m*PCSK9* (rAAV8/D377Y-mPCSK9), followed by 16 weeks of HFD (Research Diet, cat. D12079B). At the time point of the AAV injection, WT and *Txnip* KO mice and SMC^{WT} & SMC^{KO} mice were 8–10 weeks old, and the mice in the bone marrow transplantation experiment were 14–16 weeks in age due to recovery periods. Per mice, 1.0×10^{11} viral genome (vg) titer of AAV in 200 μl sterile PBS were injected via intraperitoneal injection. A previous study reported that upon AAV8-PCSK9 injection, female mice showed impaired liver *PCSK9* transduction with insufficient hypercholesterolemia.[56] In addition, to exclude possible hormonal effects (e.g., estrogen), we used only male mice in all the experiments. Mice were randomly distributed to each group. According to the exclusion criteria established prior to the experiment, mice with a total serum cholesterol of less than 500mg/dl after 16 weeks of HFD were excluded from the analysis.

Bone marrow transplantation

Bone marrow (BM) cells were collected from the femur, tibia, and humerus of WT or *Txnip* KO mice by flushing RPMI media (supplemented with 10% FBS) into the medullary cavity using a 23G needle under sterile condition. The collected BM cells were sequentially washed with serum-free RPMI and PBS through centrifugation (300 g, 7 min) and resuspension. Approximately $5.0–5.3 \times 10^6$ BM cells from WT or *Txnip* KO mice were injected intravenously via retro-orbital route into lethally irradiated (500 rad twice, 3 h interval) WT mice.

Subsequently, the mice were fed water containing antibiotics (7.6% enrofloxacin) and monitored for six weeks, until the transplanted BM was effectively reconstructed. The transplantation of BM cells was verified by blood PCR. Sequence of the primer pairs, amplicon sizes, and PCR cycle information are provided in the Major Resources Table.

Necropsy, tissue preparations, and histological staining of atherosclerotic lesions

The mice were sacrificed by CO_2 gas inhalation, and blood was obtained through cardiac puncture to measure the serum total cholesterol, triglycerides, HDL, LDL, and Ca^{2+} concentrations. The mice were perfused with phosphate-buffered saline (PBS) through the heart to eliminate blood. The hearts and whole aortas were collected. After peri-adventitial tissue removal, the hearts and aortas were briefly fixed in 10% neutralized formalin for 2 h. The hearts were molded in optimal cutting temperature (OCT) compounds for cryosectioning of the aortic sinus. The aortas were opened longitudinally and pinned onto the plate in a "Y" shape for *en-face* analysis.

The cryosections (7 μm) perpendicular to the aortic sinus were made sequentially from the sinotubular junction (start point; just before the aortic cusps appear) to the point where all the aortic cusps met (end point). From this, approximately 70–80 serial sections spanning 490–560 μm of the aortic sinus were made. For Oil Red O staining, Oil Red O dye (Sigma-Aldrich, cat. O0625) were dissolved in isopropanol, and diluted in D.W. (3: 2 ratio) and filtered to make a working solution. Slides were incubated 5 min with 100% propylene glycol, and stained with the working solution for 10 min at 60°C. After differentiating the slides by incubating in 85% propylene glycol for 1 min, the slides were washed with D.W. and mounted with glycerol. For Alizarin Red staining, Alizarin Red S dye (Sigma-Aldrich, cat. A5533) was dissolved in D.W. (0.02 g/ml concentration). Slides were incubated with Alizarin Red working solution for 5 min, and washed sequentially in acetone, acetone-xylene (1:1), xylene solutions by repetitive dipping (> 20 times), and mounted. Masson's trichrome staining was performed according to the general procedure Briefly, slides were rehydrated and fixed in Bouin's solution for 1 hour at 56°C. After washing, the slides were then stained with Weigert's iron hematoxylin working solution for 10 min. After washing with warm tap water, the slides were stained with Biebrich scarlet-acid fuchsin solution for 10 min, washed with D.W., and differentiated in phosphomolybdic-phosphotungstic acid solution for 15 min. The slides were then transferred directly into aniline blue solution and stained for 10 min. After a brief rinse, the slides were differentiated in 1% acetic acid for 5 min. The slides were then washed with D.W., dehydrated,

and mounted. Alcian Blue staining was performed using Alcian Blue Stain Kit (VECTOR, cat. H-3501) following manufacture`s instructions. Briefly, slides were incubated with acetic acid solution for 3 min, and tipped off to remove the excess, then incubated with Alcian Blue Solution for 30 min at RT. After a brief wash (~ 30 sec) with acetic acid solution, the slides were washed with D.W. and applied by Nuclear Fast Red solution for 5 min. After washing, the slides were dehydrated and mounted. For quantification of the Oil Red O, Masson`s trichrome and Alican Blue staining, 5 points of regular intervals from the start to the end of the aortic sinus sections were measured and averaged. MOMA-2, SM22α, ACAN, and CHAD proteins were visualized by immunostaining on cryosections. For the HRP detection method (MOMA-2 and SM22α), the sections were pretreated with H_2O_2 to deplete endogenous peroxidase. For the fluorescence detection method (ACAN and CHAD), auto fluorescence signals were quenched using a TrueBlack® Lipofuscin Autofluorescence Quencher (Biotium, cat. 23007) prior to the blocking step. The primary antibodies against anti-MOMA-2 (Abcam, cat. ab33451; 1:400 dilution), SM22α (Abcam, cat. ab10135; 1:200 dilution), ACAN (Proteintech, cat. 13880-1-AP; 1:200 dilution), and CHAD (Atlas Antibodies, cat. HPA018241; 1:200 dilution) were incubated at 4 °C overnight. Anti-rat (VECTOR, cat. MP-7444-15) and anti-goat (cat. MP-7405) HRP-conjugated secondary antibodies were applied to appropriately matched primary antibodies. Subsequently, the signals were detected using DAB peroxidase (VECTOR, cat. SK-4105). Anti-rabbit Alexa 488 fluorescent secondary antibodies (Jackson ImmunoResearch, cat. 711-545-152; 1:400 dilution) was applied to ACAN and CHAD. The signals were analyzed using a confocal fluorescence microscope (Zeiss, LSM800). In the case of MOMA-2 and SM22α staining, antibody signals were verified by confirming the presence of positive signals in the appropriate targets (i.e., monocytes/macrophages/foam cells for MOMA-2 and aortic media for SM22α) and the absence of signals in off-targets (e.g., cardiomyocytes/aortic media for MOMA-2 and cardiomyocytes for SM22α). In addition, background signals were checked using primary antibody-omitted controls (i.e., secondary antibody-only). For ACAN and CHAD staining, antibody signals were verified using rabbit IgG isotype controls (Cell Signaling, cat. CST3900) and secondary antibody-only controls. For the quantification of immunostaining, three regular interval points from the start to the end of the aortic sinus sections were measured and averaged. Image J software was used for quantification of histological stainings.

Measurement of the total calcium contents of atherosclerotic aortas

Total calcium contents of the atherosclerotic lesions of WT and *Txnip* KO mice were measured

using the QuantiChrom calcium assay kit (BioAssay Systems, Cat. DICA-500) with reference to the previous method.[57] The regions from the aortic sinus to the aortic arch were decalcified through overnight incubation in 300 μl of 0.6N HCl at 4°C. Next, 5 μl of supernatant were transferred to a 96-well plate and 200 μl of the working solution was mixed with reagent A and B (1:1 ratio) were added. The mixed samples were incubated for 3 min at RT and absorbance was measured at 612 nm using a microplate reader. The calcium content was normalized to the tissue dry weight.

qRT-PCR

The total RNA was extracted from the mouse aorta, adventitial layer-removed atherosclerotic lesions, or cultured VSMCs using the Hybrid-R^{TM} kit (GeneAll, cat. 305-101), according to the manufacturer's instructions. Complementary DNA was synthesized from 200–1,000 ng of total RNA using a QuantiTect Reverse Transcription kit (Qiagen, cat. 205311), and then analyzed by qPCR using a Rotor-Gene SYBR Green PCR kit (Qiagen, cat. 204074). Sequence of the qRT-PCR primer pairs, amplicon sizes, and PCR cycle information are provided in the Major Resources Table.

Randomization and blinding in *in vivo* experiments

All randomization processes used in the experiments were performed through the random number generating method using the RAND() function in Microsoft Excel. In the WT/*Txnip* KO and SMC^{WT}/SMC^{KO} experiments, mice of each genotype group were randomly allocated to cages. In the case of BMT experiment, WT mice were randomly assigned to either BM^{WT} (receiving BM from WT mice) or BM^{KO} (receiving BM from *Txnip* KO mice) groups. Mice cages of each genotype were randomly placed in the animal facility to minimize possible location-derived nuisance variables. Except for the scRNA-seq experiment, mice were given random numbers generated by a third person at the time of the sacrifice/sample collection. Necropsies and sample collections were performed according to the random number order. For blinding procedure, the random numbers were concealed to a person who conducting the experiments and/or analysis, which include the lipid measurement, histological quantification, total calcium measurement, and qRT-PCR experiment, until the final data collection.

Preparation of scRNA-seq experiment

For the scRNA-seq experiment, we used the regions from the aortic sinus to the arch, as this area consists of advanced plaques that are expected to be rich in calcification. To ensure a

sufficient cell number and biological reproducibility, four mice were pooled for each WT and *Txnip* KO genotype. Mice with plasma CHO concentrations higher than 1000 mg/dl at the 8 weeks of atherosclerosis induction were chosen for the scRNA-seq experiment to ensure adequate induction of advanced atherosclerotic lesions. The cardiac muscles and peri-adventitial tissues were removed. The aortas were subsequently incubated for 12 min in enzymatic solutions consisting of PBS with Ca^{2+} and Mg^{2+} containing 1 mg/ml of collagenase II (Worthington, cat. CLS-2) and 0.17 mg/ml of elastase (Worthington, cat. LS002279) to remove the adventitia. After the physical separation of the adventitia, the lumen was opened, and the aortic valves were removed. The aortic tissues consisting of plaque and media were cut into 2–5 mm pieces and incubated at 37 °C for 70 min with gentle shaking in a PBS solution (Ca^{2+} and Mg^{2+}) containing DNase I (90 U/mL, Sigma-Aldrich, cat. DN25), collagenase I (675 U/mL, cat. C0130), collagenase XI (187.5 U/mL, cat. C7657), hyaluronidase (90 U/mL, cat. H1115000). The resulting single-cell suspensions were filtered through a 70 μm cell strainer, stained with propidium iodide (PI), and sorted on a BD FACS Aria III instrument. After excluding the debris and doublets using forward/side scatter parameters, the PI-negative live cells were subjected to scRNA-seq experiments. 1.35×10^5 and 1.44×10^5 live single cells of WT and *Txnip* KO each were obtained and proceeded to gel bead-in-emulsion (GEMs) construction.

Pre-processing of the scRNA-seq data

Live single cells obtained from the FACS sorting were proceeded to GEM construction to target a single-cell resolution of 10,000 cells. The cDNA libraries were constructed using the Single Cell 3' Reagent Kit v3 (10x Genomics) and sequenced on the Illumina® system according to the manufacturer's instructions. The 10X Genomics libraries were de-multiplexed and quantified using the CellRanger program (ver. 1) following the manufacturer's instructions. The scRNA-seq data are available in the Sequence Read Archive (SRA) repository under the accession number SRP346850. The gene expression level of each barcode was calculated using the "quant" module of CellRanger with GRCh38 and mm10 (ver. 3.1.0). To obtain viable cells, knee plots were drawn using default CellRanger count. Two knees were detected. First knee determined 30,445 and 24,349 cells, and the second knee determined 7,186 and 11,852 cells for WT and *Txnip* KO each. Cells that passed the second knee were proceeded to further filtration. Cells with high mitochondrial gene UMI counts (≥ 30%) were considered apoptotic cells and excluded from analysis. Cells with low nFeatures or low total nCounts were removed by a heuristic method based on their distribution. Through these filtration processes, 622 and

590 low-quality cells in WT and *Txnip* KO each were excluded, resulting in 6,564 and 11,262 cells for WT and *Txnip* KO each.

Analysis of scRNA-seq data

A total of 17,826 (6,564 for WT and 11,262 for *Txnip* KO) viable cells were preprocessed using "preprocess_cds()," and then integrated using "align_cds()" in the monocle 3 package.[58] The sample batch corrections were performed using the same function. Statistical test was performed on the 21,936 commonly expressed genes in both WT and *Txnip* KO with the criteria of |average log2 fold change| > 0.1 & adjusted p-value < 0.05 to find DEGs between the two groups. The scRNA-seq data of WT and *Txnip* KO mice were visualized through UMAP. According to the developer guide of monocle 3, the cluster was divided by cutoff with the resolution of the default value $1e^{-4}$. To estimate the proportions of cells in each cluster, the scale factor (10,000 cells) was multiplied by each genotype. Cluster specific marker gene was defined as specificity ≥ 0.3 and ordered by marker_score using "top_markers()" function in monocle 3.

To integrate the normal VSMCs into WT/*Txnip* KO scRNA-seq data, the scRNA-seq data of 79 aortic arch (AA) and 64 descending thoracic aorta (DT) cells in normal mice were collected from GSE117963 of Dobnikar L et al.[28] To integrate the smooth muscle cell lineage traced atherosclerotic lesional cells into WT/*Txnip* KO scRNA-seq data, scRNA-seq data of atherosclerotic plaque cells containing ZsGreen1-labeled VSMCs (*ROSA26*$^{ZsGreen1/+}$; *Ldlr*$^{-/-}$; *Myh11-CreER*^{T2}) were sourced from GSE155513 of Pan et al.[14] The datasets consist of 4 time points (0, 8, 16, and 26 weeks of atherosclerosis induction), and all time points were integrated into our WT and *Txnip* KO scRNA-seq data. The preprocessing of scRNA-seq was conducted in the same manner as the other datasets. The integrations were performed using the "align_cds" function of monocle3 package in R. Among the 24,683 genes expressed in the WT and *Txnip* KO dataset and 15,549 genes expressed in the Pan et al. dataset, 15,528 commonly expressed genes were analyzed. The top five genes of each cell type was selected by the "top_markers" function.

For the further analysis of VSMC-derived cells, VSMCs, modulated VSMCs, and osteochondrogenic clusters were selected and re-aligned using the monocle3 package in R. Subclustering was performed in the same manner as the previous clustering method. The comparison of gene expression levels between WT and *Txnip* KO mice was performed using "FindMarkers" in the Seurat package. DEGs were defined as |average log2 fold change| ≥ 0.2

and adjusted P value < 0.05. The functional enrichment analysis for each gene set was performed using "enricher()" in the clusterProfiler package with the KEGG pathway database. The significantly associated function of each gene set was defined as a q-value < 0.2. To estimate the activity of Smad1 and Smad4 regulons (defined as transcription factor-target relationship), we used the DoRoTheA program from a previous study and followed the instructions.[40] According to the study, candidate target genes for a specific transcription factor are assigned ranging from highest confidence level (A) to lowest level (E), based on the integrated information from manual curation repositories, ChIP-seq data, computational prediction of TF binding on gene promoters, and/or predicted from large gene expression data sets. The confidence levels A, B, and C target genes were only included in our analyzed regulon (Table S9). To estimate the activity of Wnt/β-catenin regulons, gene sets consisting of Wnt/β-catenin targets were collected from previous studies and are described in Table S10.

In situ hybridization

In situ hybridizations were performed on paraffin-embedded mice aortic sinus tissues or human endarterectomized atheroma samples using RNAscope® 2.5HD Duplex Assay (Advanced Cell Diagnostics, cat. 322435). This assay enables co-detections of two different transcripts using C1 (green signal) and C2 (red signal) channels. Probes for mouse *Ly6a* (RNAscope® Probe-Mm-Ly6a-C2; cat. 427571-C2), *Myh11* (Probe-Mm-Myh11; cat. 316101), *Ibsp* (Probe-Mm-Ibsp-C2; cat. 414401-C2), and *Acan* (Probe-Mm-Acan; cat. 439101) were used. The experiments were conducted according to the manufacturer's instructions. Briefly, sections were deparaffinized, treated with H_2O_2, and proceeded to RNAscope® target retrieval procedure and protease treatment. After incubation of the probes, AMPs (amplifiers) 1-6 were sequentially incubated, and C2 signals (red) were detected. Then AMP 7-10 were sequentially incubated and C1 signals (green) were detected. Counterstains were performed using hematoxylin. *Polr2a & Ppib* (constitutively expressed genes of mouse, RNAscope® 2.5HD Duplex Positive Control Probe (Mm) PPIB-C1/POLR2A-C2 cat. 321651) and *DapB* (constitutively expressed genes of *E. coli*, Negative Control Probe-DapB, cat. 310043) were used as positive and negative control probes, respectively. Three points of regular intervals from the start to the end of the aortic sinus sections were measured and averaged for quantification. In human sections, probes for *IBSP* (Probe-Hs-IBSP; cat. 587221) and *HAPLN1* (Probe-Hs-HAPLN1; cat. 506171) were used. As only C1 channel was used, amplification steps using AMP 4-7 were omitted according to the manufacturer`s guide. *PPIB* (Probe-Hs-PPIB; cat. 313901) was used as positive control probes for human sections.

Sequential staining and merging of Alizarin Red staining and Alcian Blue staining on same paraffin sections.

For analyzing spatial relationship between calcified area and cartilage metaplasia area in atherosclerotic lesions, sequential staining of Alizarin Red and Alcian Blue were performed on the same paraffin sections. The slides were first stained with Alizarin Red staining and the resulting microscopic images were taken. Then the coverslip was removed by incubating the slides in xylene for > 1 day. The slides then rehydrated by incubating sequentially in ethanol and D.W., and proceeded to Alcian Blue staining. The Alizarin Red staining was eventually, near-completely removed during the rehydration step and the acetic acid solution-applying step of Alcian Blue staining. Microscopic images of Alican Blue staining were taken. The Alizarin Red-stained images and Alcian Blue-stained images of the same areas were merged using Photoshop software (Adobe, ver. 23.4.2). Specifically, Alizarin Red-stained images were overlaid on Alcian Blue-stained images, and precisely synchronized using the Edit-Transform function of Photoshop. Then the background of Alizarin Red-stained images were normalized to white using the Curve function. Next, Alizarin Red-positive red signals were extracted using the Select-Color Range function, and overlaid on the Alcian Blue-stained images. Lastly, the extracted red signals were converted to grayish-scale using the Black & White function.

Integration of the human and mouse scRNA-seq data

For the integration of human and mouse scRNA-seq data, cells of VSMCs and fibroblast-like clusters were obtained from scRNA-seq data from a total of 48 patient samples across four previous studies (GSE155512,[14] n = 3, 3,117 cells; GSE159677,[23] n = 3, 9,511 cells; GSE131780,[29] n = 4, 4,465 cells; Slenders et al,[35] n = 38, 43,290 cells) and then integrated them with 13,596 cells of VSMC, modulated VSMC, osteochondrogenic, and fibroblast-like clusters of WT mice. The preprocessing of scRNA-seq was conducted in the same manner as the other datasets. The integrations were performed using the "align_cds" function of monocle3 package in R. In this case, only human and mouse homologous genes were used (the homologous genes were previously defined according to 'Mouse/Human Orthology with Phenotype Annotations' of the Jackson Laboratory, http://www.informatics.jax.org).

Analysis of human scRNA-seq data GSE159766

The scRNA-seq data GSE159677 consisted of type VII calcified atherosclerotic plaque cores matched with the adjacent proximal regions of three human patients.[23] Downsampling was performed to reduce data bias due to differences in the cell number (# cells per sample = 2,500).

The *MYH11* and *ACTA2* positive cluster cells (VSMCs) were collected from GSE159677. The selected VSMCs were processed by the same procedure in the mouse data. Four subclusters (VSMCs, modulated VSMCs, osteochondrogenic, and fibroblast-like) were characterized by the markers in the mouse scRNA-seq data.

Immunostaining of human atherosclerotic lesion samples

Endarterectomized atherosclerotic plaque tissues from the carotid artery region, which harbored calcification were obtained from patients. The tissue samples were fixed in 10% neutral buffered formalin, processed in a routine procedure, and embedded in paraffin. Serial sections (3 μm) were obtained and subjected to either hematoxylin & eosin staining or immunostaining. For the immunostaining of TXNIP and α-SMA, antigen retrieval was performed using a Tris-EDTA buffer (pH 9.0; Abcam, cat. ab93864). Endogenous peroxidase was depleted by incubation with H_2O_2. TXNIP (Abcam, cat. ab188865; 1:200 dilution; 0.25mg/ml concentration), rabbit monoclonal IgG (Cell signaling, cat. CST3900; 1:2000 dilution; 0.25mg/ml concentration), and α-SMA (Agilent, cat. M0851; 1:200 dilution) primary antibodies were incubated overnight at 4 °C. Anti-rabbit (VECTOR, cat. MP-7401), and anti-mouse (cat. MP-7402) HRP-conjugated secondary antibodies were applied to the appropriate slides, and the signals were produced through DAB peroxidase (VECTOR, cat. SK-4105). To quantify the intensity of TXNIP staining, images of two to three × 400 field were taken in the medial side (marked by *α*-SMA on the serial sections) of the periphery of the calcified area or non-calcified area. The staining intensity was evaluated using the ImageJ software (ver. 1.53e, NIH).

Primary VSMC culture experiment

The pooled VSMCs from two to three WT mice constituted one biological replicate. Aortas were obtained from 3 to 5 weeks of WT (C57BL6/J) mice. For adventitia removal, the aortas were incubated for 12 min in enzymatic solutions consisting of PBS with Ca^{2+} and Mg^{2+} containing 1 mg/ml of collagenase II (Worthington, cat. CLS-2) and 0.17 mg/ml of elastase (cat. LS002279). The endothelium was removed by gentle scraping. The resulting media was fully digested into single cells by 1 h 30 min to 2 h incubations of the same enzymatic combination as that used for adventitia removal. The cultured VSMCs were maintained in DMEM/high glucose supplemented with sodium pyruvate and L-glutamine (GE Healthcare Hyclone™, cat. SH30243.01) supplemented with 10% fetal bovine serum (FBS), penicillin (50 U/ml), and streptomycin (50 μg/mL) in a 5% CO_2 atmosphere at 37 °C. P3 to P4 passaged

VSMCs were used for the experiments. *Txnip* siRNA (Bioneer, AccuTarget™ Genome-wide Predesigned siRNA No. 56338-3), *Smad4* siRNA (Bionics, A10001 Pre-designed siRNAs, candidate 1), *MAPK14* siRNA (Bionics, A10001 Pre-designed siRNAs, candidate 3), or negative control siRNA (Bioneer, AccuTarget™ Negative Control siRNA, cat. SN-1012) were delivered into the cultured VSMCs using Lipofectamine RNAiMAX reagent (Thermo Fisher, cat. 13778075) to a final concentration of 10 nmol. For osteodifferentiation, the cultured VSMCs were grown in an "osteogenic cocktail," consisting of 0.25 mM L-ascorbic acid, 10 mM β-glycerophosphate, and 0.4 mM H_2O_2 in DMEM/high glucose without sodium pyruvate and L-glutamine (WELGENE, cat. LM001-03) supplemented with 10% FBS and penicillin/streptomycin. The medium was changed every 2 or 3 days. Under these conditions, osteodifferentiation was achieved in approximately 14 days. At the end point, the extent of osteodifferentiation was visualized by Alizarin Red staining and quantified using the cetylpyridinium chloride extraction method. 350 mg of cetylpyridinium chloride (Sigma-Aldrich, C0732) was dissolved in 10 ml D.W. 330 μl of a cetylpyridinium chloride solution per well was added to 48 well plate. After incubation in the dark for 30 min, the absorbance of the resulting solution was measured at 405 nm. The amount of accumulated Alizarin Red was calculated by comparing it with a standard curve. BMP2 (R&D Systems, cat. 355-BM), or K02288 (MedChemExpress, cat. HY-12278) were used at the indicated concentrations and times.

Immunoblotting

The proteins from whole cell lysates were extracted from primary cultured VSMCs using the Cytobuster™ protein extraction reagent (Millipore, cat. 71009) with a protease inhibitor cocktail (GenDEPOT, cat. P3100), and a phosphatase inhibitor cocktail (GenDEPOT, cat. P3200). Concentrations of the extracted proteins were measured using Pierce™ BCA Protein Assay Kit (Thermo Fisher, cat. 23227). Proteins were denatured using 5X SDS-PAGE loading buffer (Biosesang, cat. SF2002-110-00). To analyze the cytoplasmic and nuclear fractions of β-catenin and Smad4, the cytoplasmic and nuclear proteins were compartmentalized using the NE-PER Nuclear and Cytoplasmic Extraction Reagents kit (Thermo, cat. 78833). The proteins were separated by 10% sodium dodecyl sulfate-polyacrylamide gel electrophoresis (SDS-PAGE) and transferred to nitrocellulose membranes (Cytiva, Amersham™Protran™ 0.45μm NC, cat. 10600003). The membranes were blocked with 5% skim milk. Anti-TXNIP (Abcam, cat. ab188865; 1:500 dilution), β-catenin (Santa Cruz Biotechnology, cat. sc-17791; 1:200 dilution), α-tubulin (Cell Signaling, cat. CST2144; 1:1000 dilution), Lamin B1 (cat. ab16048;

1:1000 dilution), p-Smad1/5/9 (cat. CST13920; 1:500 dilution), Smad1 (cat. CST6944; 1:1000 dilution), Smad4 (cat. sc-7966; 1:200 dilution), Smad5 (cat. sc-101151; 1:200 dilution), Smad6 (cat. sc-25321; 1:200 dilution), Smad7 (cat. sc-365846; 1:100 dilution), p38 (cat. sc-7149; 1:200 dilution), p-p38 (cat. CST4511; 1:500 dilution), Smurf1 (cat. sc-100616, 1:200 dilution), Smurf2 (cat. CST12024, 1:1000 dilution), BMPR1A (cat. sc-134285, 1:200 dilution), HA-tag (cat. CST3724, 1:1000 dilution) and GAPDH (cat. sc-365062; 1:500 dilution) primary antibodies were incubated at 4 °C overnight. For the co-immunoprecipitation experiments, Smad5 (cat. sc-101151) and Smad7 (cat. sc-25321) antibodies were substituted for rabbit-host antibody Smad5 (cat. CST12534; 1: 1000 dilution) and Smad7 (Bioss, cat. bs-0566R, 1: 200 dilution) to avoid eluted mouse antibody fragments from anti-HA-tag beads. Subsequently, anti-mouse or anti-rabbit HRP-linked secondary antibodies (Cell Signaling, cat. CST7076 and CST7074) were incubated at RT 1hour with the appropriate primary antibody host. The signals were produced using a chemiluminescent HRP substrate (Merck Millipore, cat. WBKLS0500) and analyzed using ImageQuant LAS 4000 Mini (GE Healthcare). If necessary, the membranes were stripped using Restore™ Western Blot Stripping Buffer (Thermo Fisher, cat. 21059), followed by additional blotting.

Co-immunoprecipitation

pCMV3 vector containing c-terminal HA-tagged mouse TXNIP cDNA clone (SinoBiological, cat. MG52103-CY) or control vector (SinoBiological, cat. CV013) were transfected into primary cultured VSMCs using Lipofectamine LTX with Plus Reagent (Thermo Fisher, cat. 15338030). 2500 ng of plasmid DNA were transfected per one 6 well, or proportionally scaled up. Co-immunoprecipitation was performed using Pierce™ HA-Tag Magnetic IP/Co-IP Kit (Thermo Fisher, cat. 88838) following manufacturer`s instruction. Briefly, cells were lysed with IP Lysis/Wash Buffer and debris were removed by centrifugation. Resulting cell lysates were incubated with anti-HA-Tag Magnetic Beads. After a series of washing steps, captured proteins were eluted by boiling with a non-reducing sample buffer. Then eluted proteins were reduced by adding DTT and proceeded to immunoblotting.

Statistics

Statistical analyses were performed using GraphPad Prism software ver. 7. All the data are presented as mean ± standard deviation. In *in vivo* experiments, the Shapiro-Wilk normality tests were performed to test whether data follows a Gaussian distribution, except for groups with small n ($n < 6$). An unpaired Student's t-test (two-tailed) was applied for parametric data.

The Mann–Whitney *U*-test (two-tailed) was applied for non-parametric data and the groups with $n < 6$. In *in vitro* experiments, we assumed that the data follows a Gaussian distribution by relying on the central limit theorem. An unpaired Student's t-test (two-tailed) was applied for comparing two groups, and a one-way ANOVA followed by a post hoc analysis specified by the GraphPad Prism software was applied for comparing more than two groups. The statistical significance was set at $P \leq 0.05$. Representative images were chosen to represent the mean of quantification for each group. Statistical information including the *n* of each group, the normality test results (if applied), the applied statistical methods and *P* values for each figure are summarized in the Table S11.

Study approval

Human endarterectomized atherosclerotic plaque samples were obtained from patients after the receipt of written informed consent in accordance with the Declaration of Helsinki. The study protocol was approved by the Institutional Review Board of Hanyang University Hospital, Seoul, Korea (IRB number: 2021-11-027-001). All the animal experiments were approved by the Institutional Animal Care and Use Committee (IACUC) of Seoul National University (approval numbers: SNU-180612 and 210517).

Supplemental Figures and Figure Legends

Figure S1

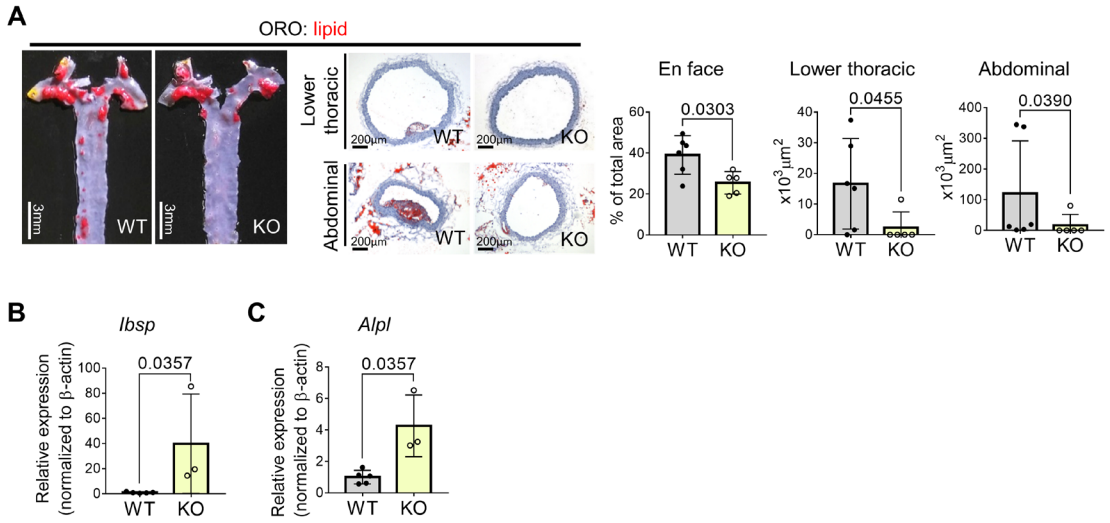

Figure S1 (related to Figure 1). Lesions size measurement and qRT-PCR results of bone marker genes in the aorta of WT and *Txnip* KO mice. The atherosclerotic burden of aortas was analyzed by making *en face* preparation (aortic arch–upper thoracic) and serial cryosections (lower thoracic and abdominal) (**A**, n = 6/5). The aortas of remaining mice were used for qRT-PCR (**B**, n = 5/3) (see Figure 1A). **A**, Representative images showing Oil Red O (ORO)-stained *en faced* and cryosectioned aorta, and quantification results of the lesion size. **B**, qRT-PCR results of *Ibsp* and *Alpl* from the atherosclerotic aortas of WT and *Txnip* KO mice. The applied statistical tests and results are summarized in the Table S11. The error bars denote standard deviation. The exact P values are specified.

Figure S2

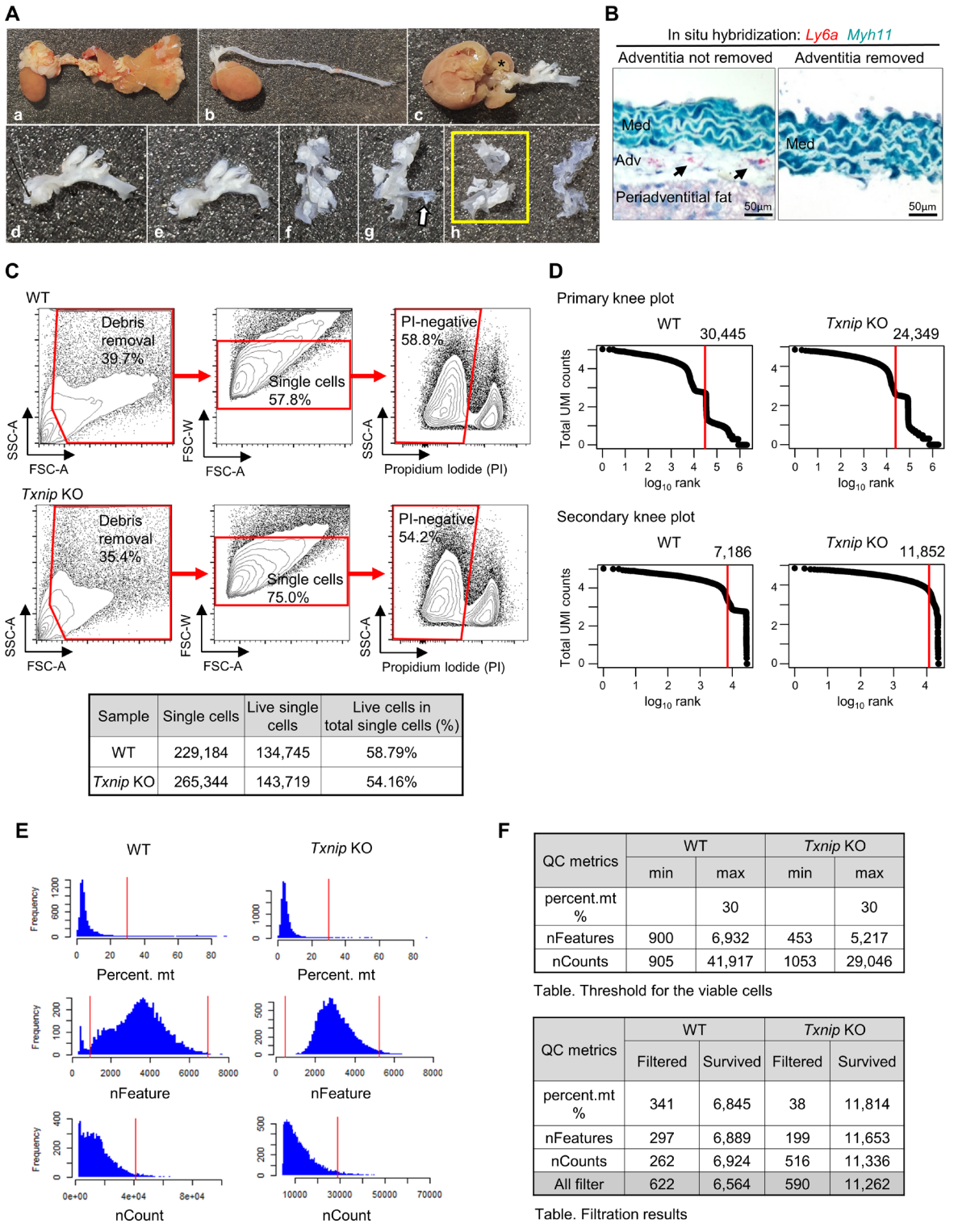

Sample	Single cells	Live single cells	Live cells in total single cells (%)
WT	229,184	134,745	58.79%
Txnip KO	265,344	143,719	54.16%

F

QC metrics	WT		*Txnip* KO	
	min	max	min	max
percent.mt %		30		30
nFeatures	900	6,932	453	5,217
nCounts	905	41,917	1053	29,046

Table. Threshold for the viable cells

QC metrics	WT		*Txnip* KO	
	Filtered	Survived	Filtered	Survived
percent.mt %	341	6,845	38	11,814
nFeatures	297	6,889	199	11,653
nCounts	262	6,924	516	11,336
All filter	622	6,564	590	11,262

Table. Filtration results

Figure S2 (related to Figure 2). Preparation and pre-processing of scRNA-seq experiments. A, Representative photographs showing sample preparation procedure. (a) Harvesting of the heart and aorta. (b) Periadventitial tissue removal. (c) Opening of the aortic sinus and removal of the aortic part below the aortic arch. (d) Removal of the heart tissue,

including the aortic valves. (e) Enzymatic digestion for adventitial removal (f) Opening of the lumen. (g) Stripping of the adventitia. (h) Completion of the adventitial removal. Resulting adventitia-removed atherosclerotic lesion (marked by yellow box) was used for scRNA-seq experiment. **B**, Confirmation of adventitial removal using *in situ* hybridization of *Ly6a* (red signal, marks adventitial *Ly6a*$^{+}$ cells) and *Myh11* (green signal, marks medial SMCs). **C**, FACS plots showing the gating scheme to obtain live single cells using forward scatter (FSC), side scatter (SSC), and PI-positive cell exclusion. **D**, Knee plots drawn by default CellRanger count settings. Two knees were called, and cells that passed the second knee proceeded to the next step. **E** and **F**, Histograms (**E**) and tables (**F**) showing the sample filtration results prior to dimensional reduction and integration of WT and *Txnip* KO scRNA-seq data. Low-quality cells were filtered out using nFeature (the number of expressed genes in each cell), nCount (total UMI counts in each cell), and percentage (percentage of the mitochondrial gene UMI counts) parameters.

Figure S3

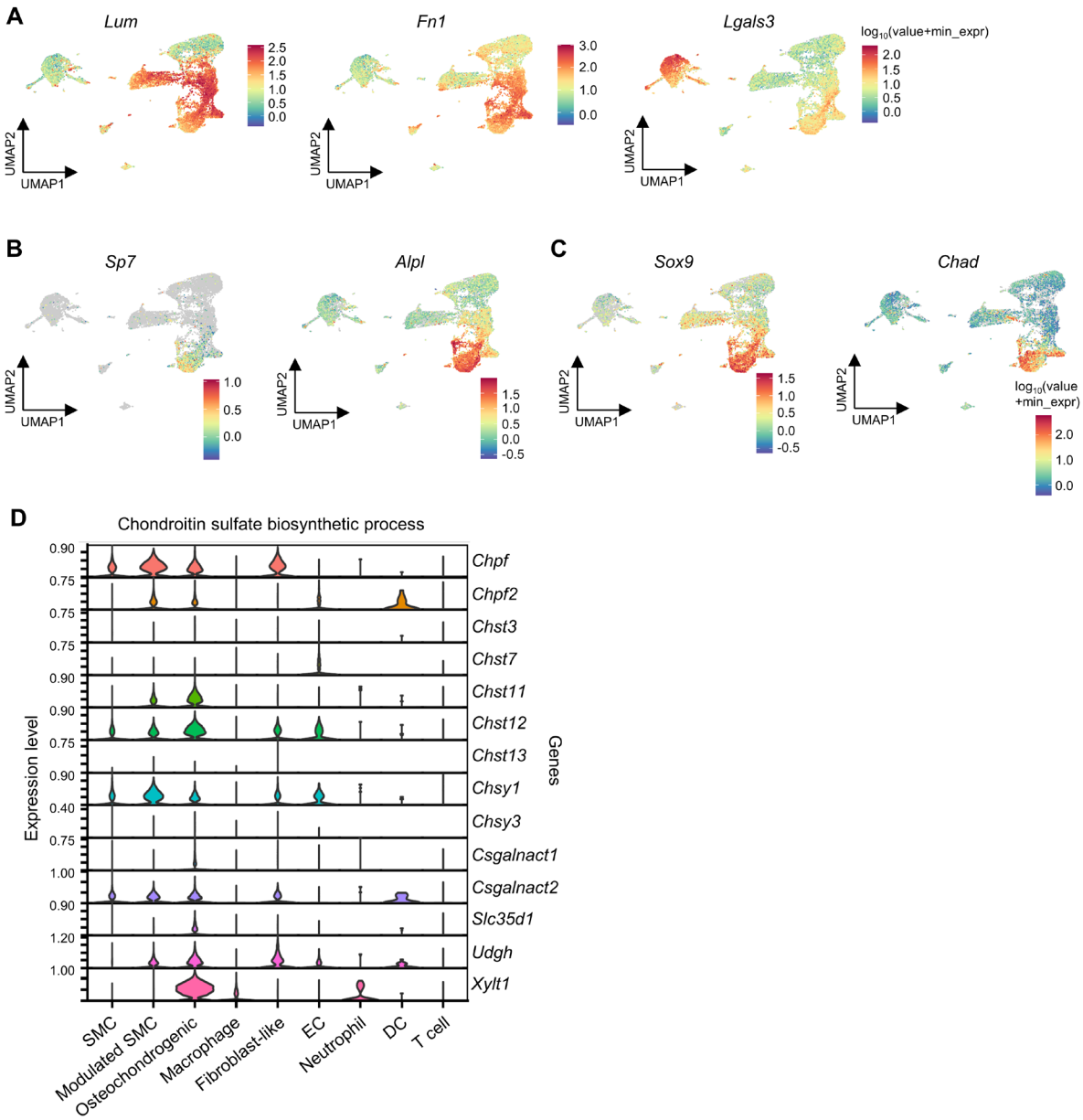

Figure S3 (related to Figure 2). Feature plots of additional marker genes for modulated VSMCs and osteochondrogenic clusters, and expression of the cartilage ECM-related genes. A, Feature plots of *Lum*, *Fn1*, and *Lgals3*. **B** and **C**, Feature plots for additional osteogenic gene *Sp7* and *Alpl*, and chondrogenic gene *Sox9* and *Chad*. **D**, Violin plots showing expressions of chondroitin sulfate biosynthetic process-related genes (GO ID: 0030206).

Figure S4

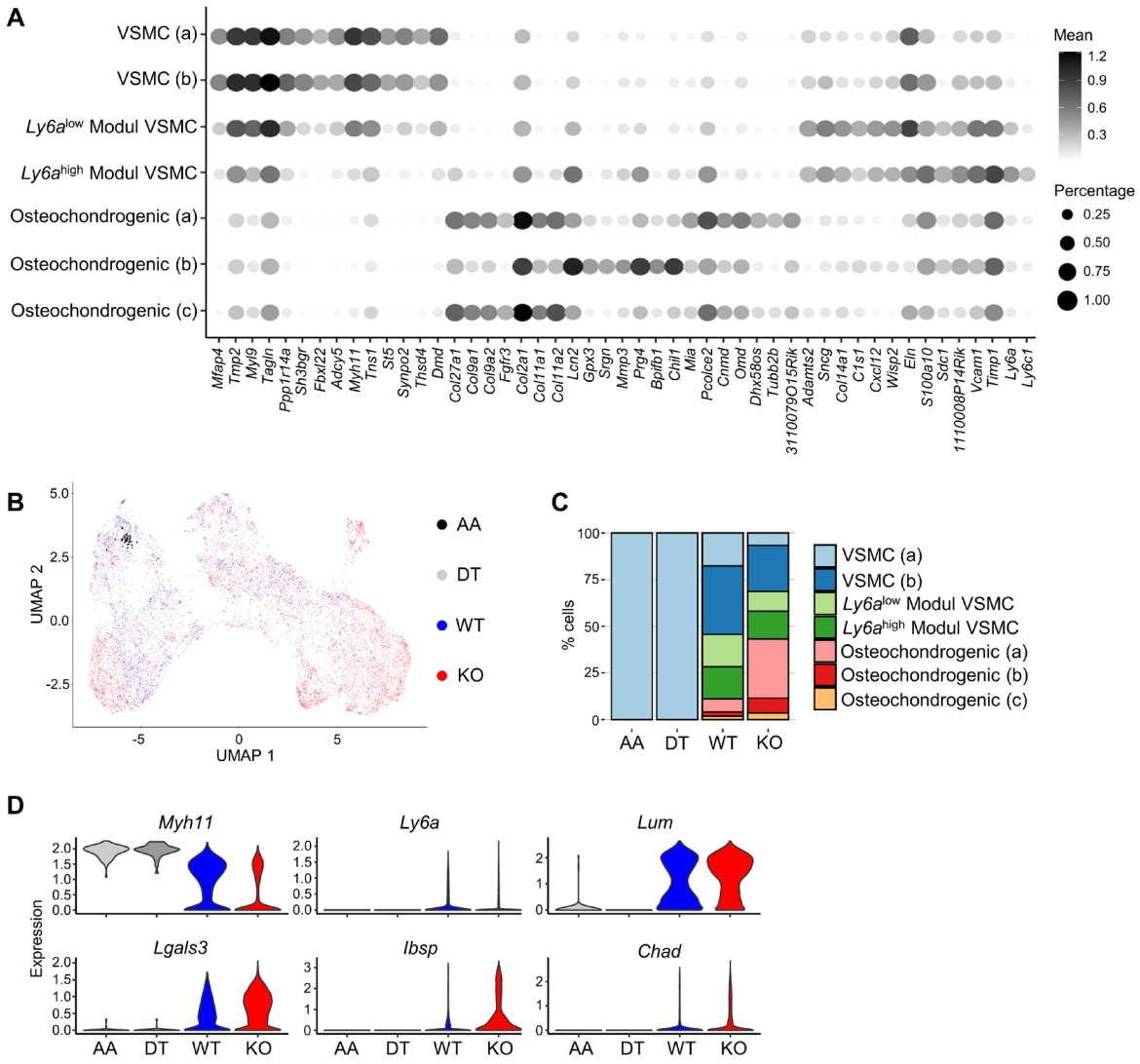

Figure S4 (related to Figure 5). Additional data related to analysis of VSMC-derived cell clusters. A, Heatmap showing the top specific genes for VSMC-derived subclusters. **B–D**, ScRNA-seq data consisting of the aortic arch (AA) and distal thoracic aorta (DT) from normal healthy WT mice (GSE1179763)[28] were integrated into WT and *Txnip* KO mice scRNA-seq data. **B**, UMAP color labeled by the samples. **C**, Cell type fraction rate of the samples. **D**, Violin plots showing expression of representative marker genes *Myh11* (VSMC cluster), *Ly6a*, *Lum* (modulated VSMC cluster), *Lgals3* (modulated VSMC~osteochondrogenic cluster), *Ibsp*, and *Chad* (osteochondrogenic cluster).

Figure S5

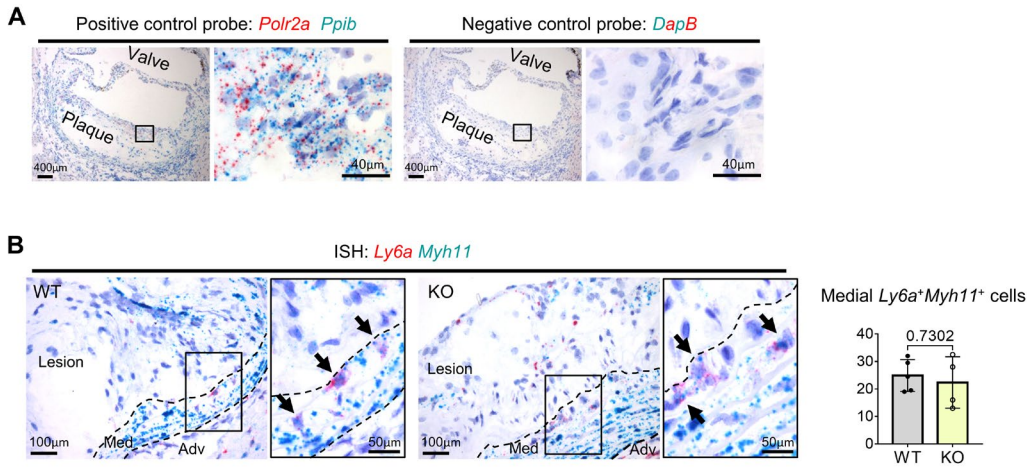

Figure S5 (related to Figure 5). Validation of *in situ* hybridization, and localization and quantification of modulated VSMCs. A, The *in situ* hybridization experiment was validated by probing *Polr2a* and *Ppib* (positive control) and *DapB* (negative control) on WT atherosclerotic lesions. **B**, Detection and quantification of medial *Ly6a*$^{+}$*Myh11*$^{+}$ cells (marked by arrows). n = 5/4 for WT/*Txnip* KO. Med, medial layer. Adv, adventitial layer. Data were analyzed using Mann-Whitney U-test (two-tailed). The error bars denote standard deviation. The exact P values are specified.

Figure S6

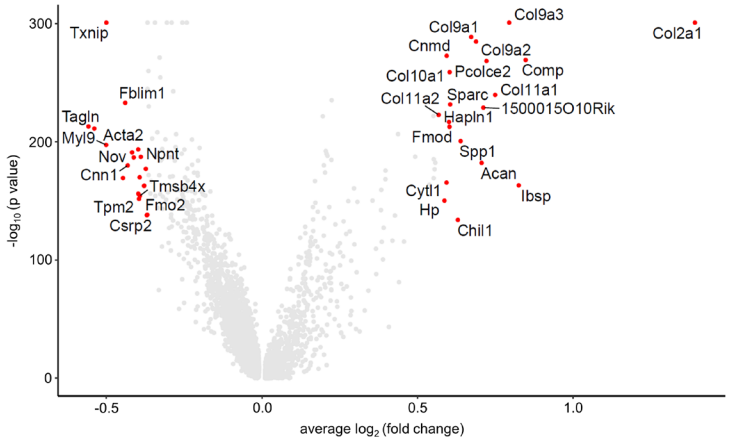

Figure S6 (related to Figure 5F). Volcano plot showing DEGs between WT and *Txnip* KO for the VSMC-derived cell population. VSMCs, modulated VSMCs, and osteochondrogenic clusters were tied together as VSMC-derived cells. The bone- and cartilage-related genes and various collagen-producing genes were highly upregulated in the VSMC-derived *Txnip* KO cells.

Figure S7

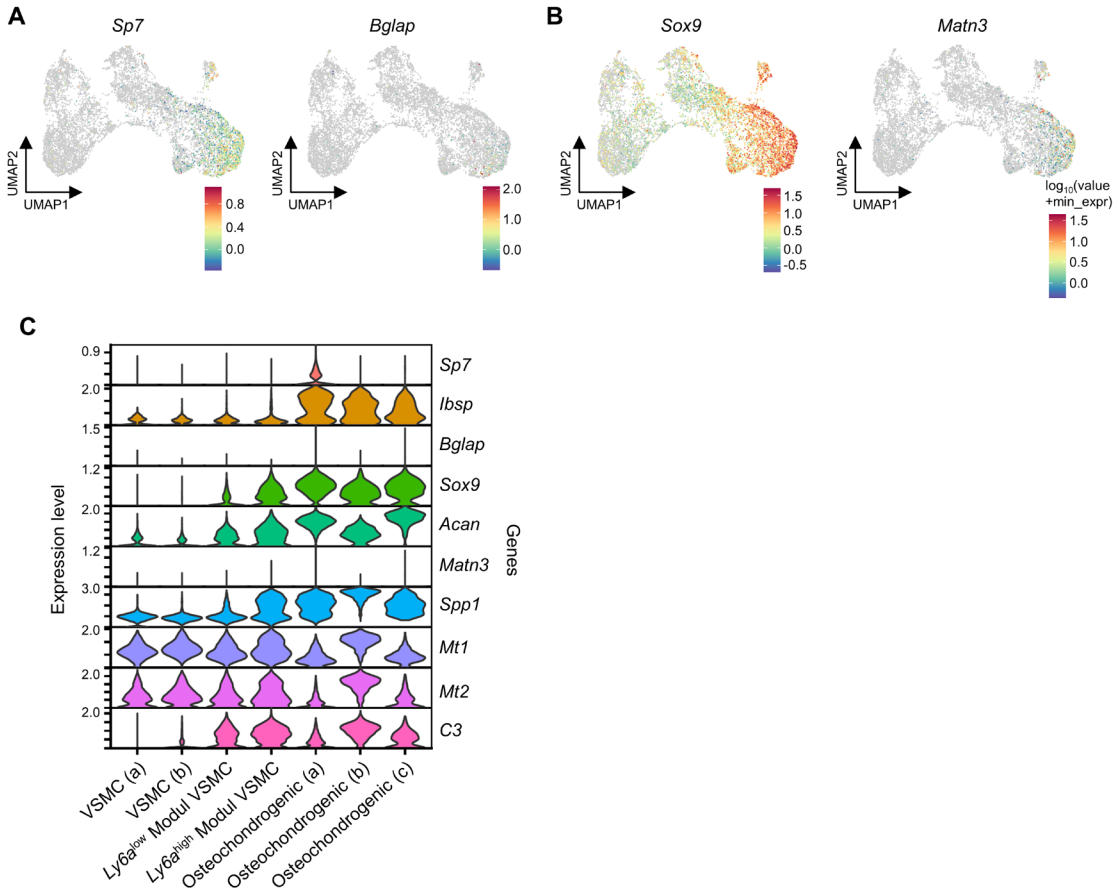

Figure S7 (related to Figure 5C and 5G). Expression patterns of additional osteogenic and chondrogenic markers. A and **B**, Feature plots for *Sp7*, *Bglap*, *Sox9*, and *Matn3*. **C**, Violin plots showing expression patterns of osteogenic genes, chondrogenic genes, metallothionein genes (*Mt1* and *Mt2*), and *C*3 in VSMC-derived clusters.

Figure S8

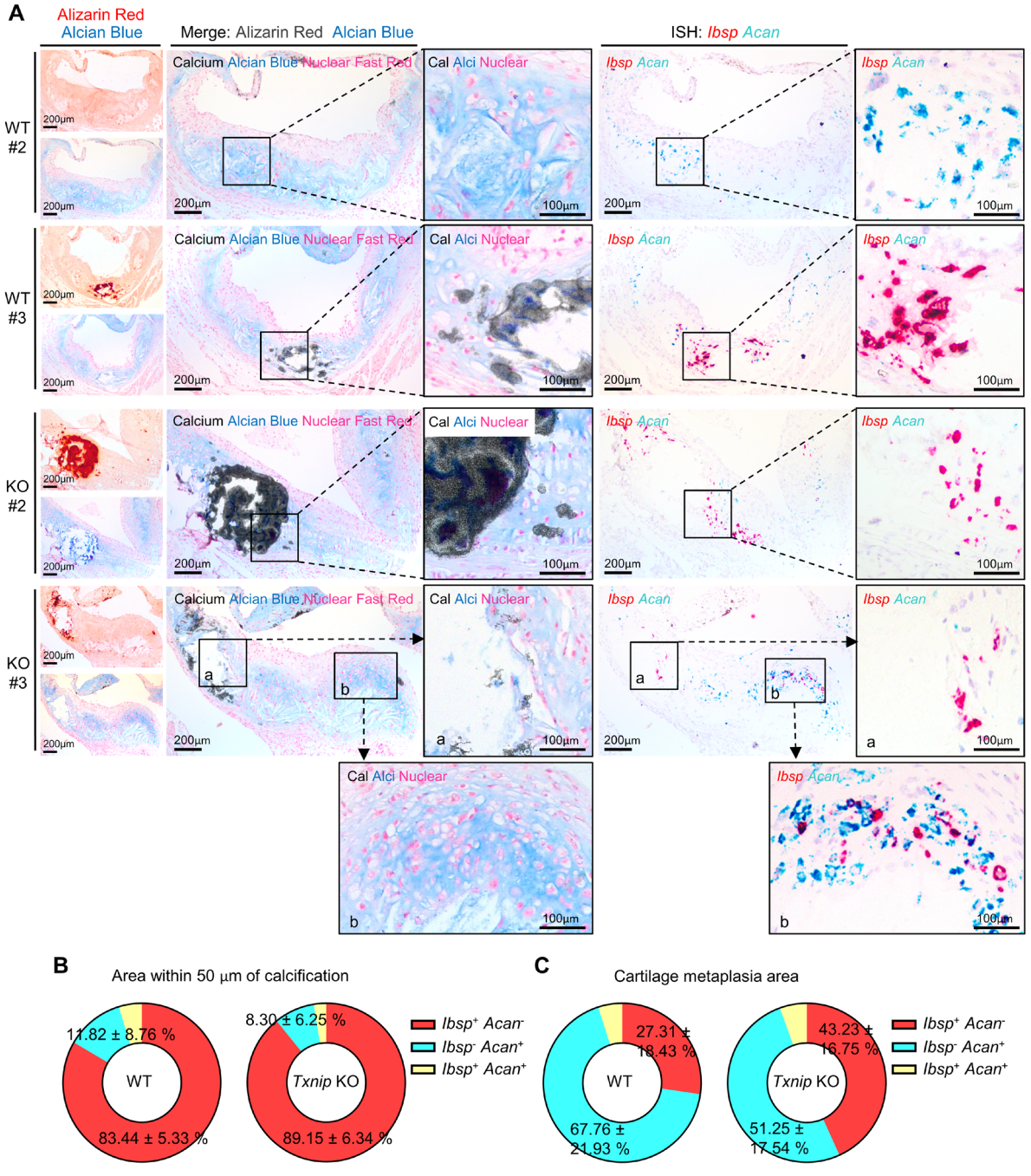

Figure S8 (related to Figure 5G). Characterizing osteogenic and chondrogenic populations. A, Additional photomicrographs related to Figure 5G. **B** and **C**, Quantification results showing localization of *Ibsp*$^{+}$*Acan*$^{-}$, *Ibsp*$^{-}$*Acan*$^{+}$, and *Ibsp*$^{+}$*Acan*$^{+}$ cells in relation to calcified foci (cells within 50 μm of Alizarin Red^{+} area) or cartilage metaplasia area (marked by lacunae-shaped cells with Alcian Blue^{+} ECM). n = 5/4 for WT/*Txnip* KO.

Figure S9

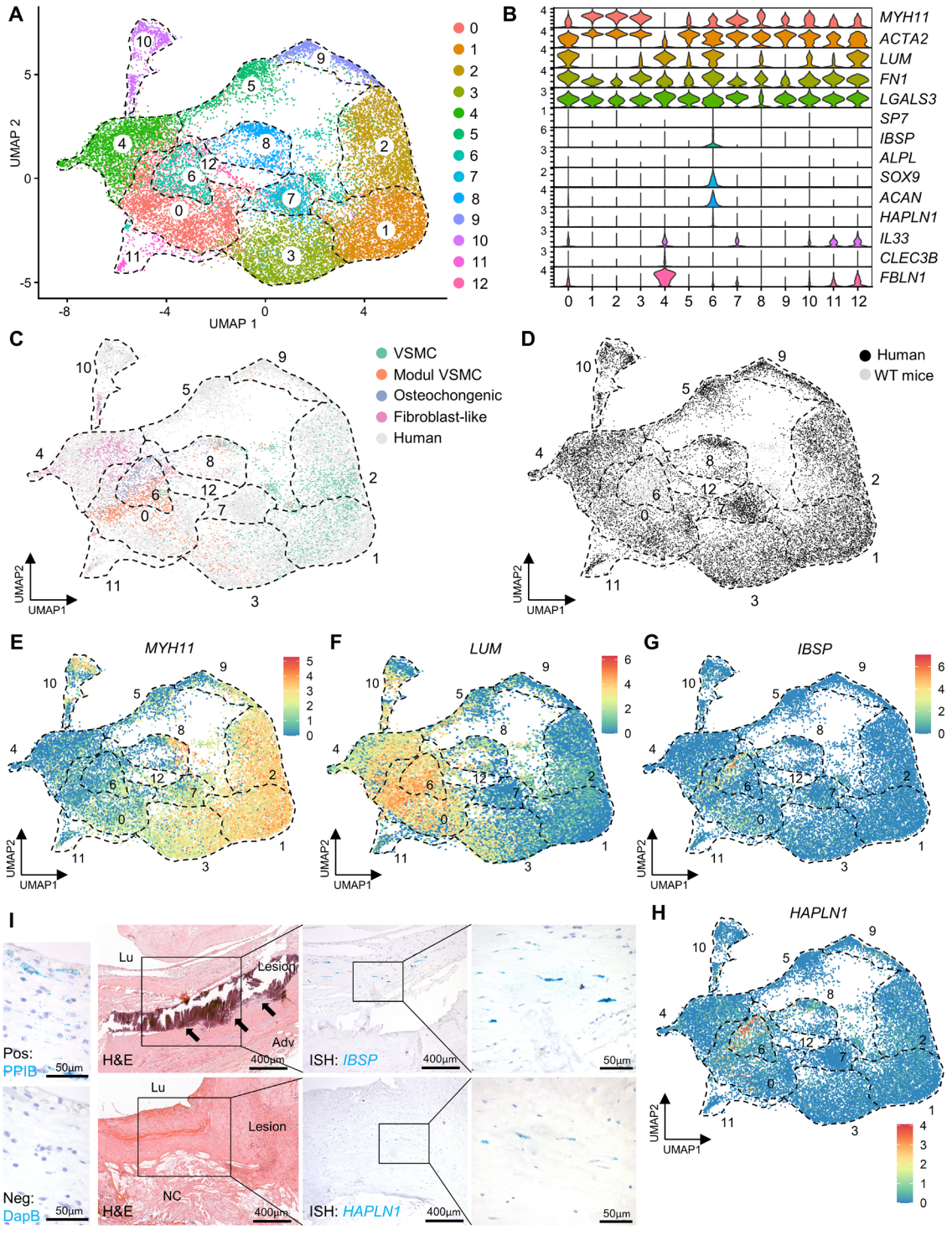

Figure S9. Existence of the modulated VSMC and osteochondrogenic population in human atherosclerotic lesions. A–H, Joint clustering result of human and mouse scRNA-seq data. VSMCs and fibroblast-like cells were obtained from scRNA-seq data from a total of 48 patient samples across four previous studies (GSE155512,[14] n = 3; GSE159677,[23] n = 3;

GSE131780,[29] n = 4; Slenders et al.,[35] n = 38) and integrated them with WT mice cells of VSMC, modulated VSMC, osteochondrogenic, and fibroblast-like cluster. **B**, Violin plots of representative marker genes. *MYH11* and *ACTA2*: VSMCs; *LUM*, *FN1* and *LGALS3*: Modulated VSMCs; *SP7*, *IBSP* and *ALPL*: osteogenic; *SOX9*, *ACAN* and *HAPLN1*: chondrogenic; *IL33*, *CLEC3B* and *FBLN1*: fibroblast-like. **C** and **D**, UMAP showing WT mice cell population (**C**) and human cells (**D**). **E–H**, Feature plots for *MYH11*, *LUM*, *IBSP*, and *HAPLN1*. **I**, *In situ* hybridization result of *IBSP* and *HAPLN1* on human atherosclerosis samples. Representative images of four samples. Pos, positive control. Neg, negative control. Lu, lumen. Adv, adventitia. NC, necrotic core. ISH, *in situ* hybridization. Arrows indicate calcified area.

Figure S10

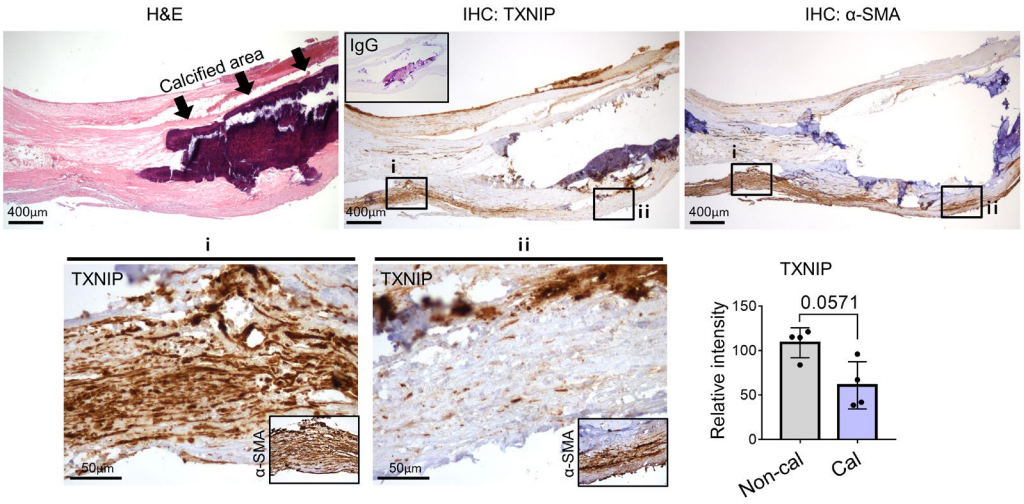

Figure S10 (related to Figure 5H). Immunohistochemistry of TXNIP in human endartertomized atheroma plaque samples harboring plaque calcification. Medial side was marked by *α*-SMA immunostaining on the serial sections. The TXNIP signals between the non-calcified and calcified areas were analyzed by Mann-Whitney *U*-test (two-tailed, $n = 4$). The exact *P* values are specified.

Figure S11

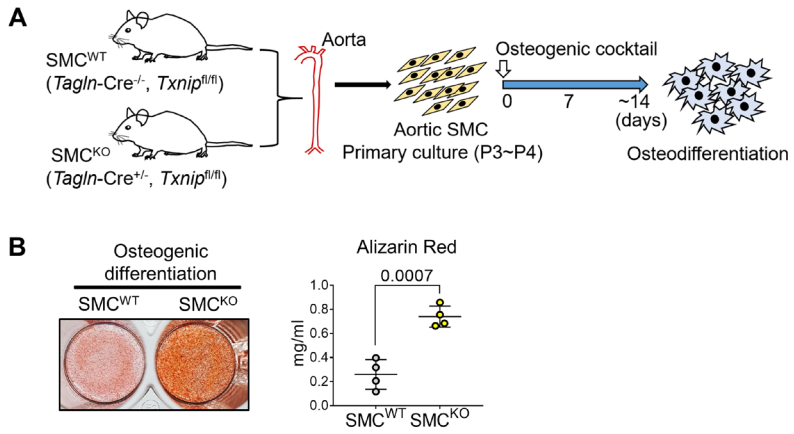

Figure S11 (related to Figure 7). Osteodifferentiation result using primary cultured VSMCs from SMC^{WT} and SMC^{KO}. A, Schematic illustration of the experiment. VSMCs were primary cultured from littermate control of SMC^{WT} and SMC^{KO}. The pooled VSMCs from two to three mice constituted one biological replicate. **B**, Alizarin Red staining results of osteodifferentiation (end point). The staining was quantified by cetylpyridinium chloride extraction. $n = 4$. The data were analyzed by an unpaired Student's *t*-test (two-tailed). The error bars denote standard deviation. The exact *P* values are specified.

Figure S12

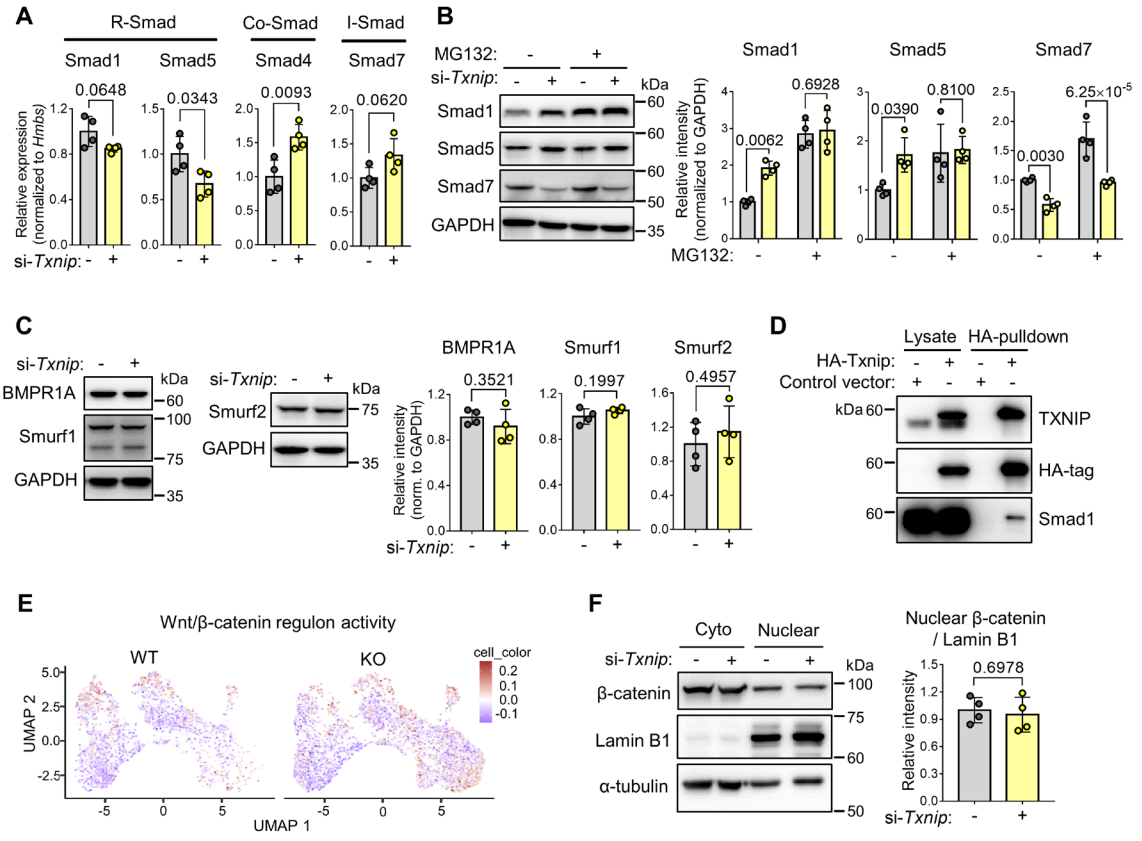

Figure S12 (related to Figure 8). Additional experimental data regarding the mechanism study. A, qRT-PCR results showing mRNA expressions of the Smad molecules which showed altered protein level upon TXNIP suppression. *Hmbs* was used as a housekeeping gene. $n = 4$. **B**, Western blot showing the MG132 treatment result to observe whether the effects of TXNIP suppression on Smad1, Smad5, and Smad7 molecule involve proteasome degradation pathway. $n = 4$. **C**, Western blot showing no effect of TXNIP suppression on BMPR1A, Smurf1, and Smurf2. $n = 4$. **D**, Co-immunoprecipitation results. Primary cultured VSMCs were transfected with pCMV3 vector containing HA-tagged TXNIP cDNA clone or control vector. Results from two independent experiments. **E** and **F**, Wnt/β-catenin signaling is not involved in the effect of TXNIP on VSMC osteodifferentiation. **E**, Feature plots showing Wnt/β-catenin regulon activity in the VSMC-derived cells of WT and *Txnip* KO mice. **F**, Western blot showing cytoplasmic and nuclear fractions of β-catenin upon *Txnip* siRNA treatment. α-tubulin and Lamin B1 were used as the loading controls for the cytoplasmic and nuclear fractions, respectively. The applied statistical tests and results are summarized in the Table S11. The error bars denote standard deviation. The exact *P* values are specified.

Supplemental Tables

Table S1-S8: Provided as a separate Excel file.

Table S9: Gene list of the analyzed Smad1 and Smad4 regulons from the DoRoTheA program.[40] The confidence levels A, B, and C target genes were selected for analysis.

Transcription factor	Confidence	Target	Transcription factor	Confidence	Target
Smad1	C	Cdkn1a	Smad4	A	Ahr
Smad1	C	Id2	Smad4	A	Apoc3
Smad1	C	Id3	Smad4	A	Bambi
Smad1	C	Spp1	Smad4	A	Bglap
Smad1	C	Tnfrsf11b	Smad4	A	Bglap2
Smad1	C	Gdf15	Smad4	A	Bglap3
Smad1	C	Zeb2	Smad4	A	Btrc
Smad1	C	Arhgef3	Smad4	A	Ccn1
Smad1	C	Arid1a	Smad4	A	Cdkn1a
Smad1	C	Ctnnb1	Smad4	A	Cdkn2b
Smad1	C	Igf2r	Smad4	A	Dach1
Smad1	C	Lyn	Smad4	A	Epo
Smad1	C	Mrps27	Smad4	A	Fshb
Smad1	C	Stk32b	Smad4	A	Fstl3
Smad1	C	Tanc1	Smad4	A	Ihh
Smad1	C	Xpo7	Smad4	A	Jun
Smad1	C	Zfp521	Smad4	A	Met
			Smad4	A	Myc
			Smad4	A	Nkx2-5
			Smad4	A	Por
			Smad4	A	Pthlh
			Smad4	A	Runx1t1
			Smad4	A	Serpine1
			Smad4	A	Smad7
			Smad4	A	Tgfb1
			Smad4	A	Tnc
			Smad4	A	Tnfrsf11b
			Smad4	A	Zfp36

Table S10: Gene list of the analyzed Wnt/β-catenin regulon. Among the known target genes of Wnt/β-catenin signaling (referenced from: https://web.stanford.edu/group/nusselab/cgi-

bin/wnt/target_genes), genes reported as direct targets of Wnt/β-catenin signaling in mammalian species were selected.

Axin2	*Ccnd1*	*Cdc25*	*Cdx1*	*Cldn1*	*Ctla4*	*Fgf18*	*Fosl1*
Fst	*Fzd7*	*Gbx2*	*Gja1*	*Id2*	*Jun*	*Krt1*	*Lef1*
Lgr5	*Myc*	*Mycbp*	*Neurod1*	*Nrcam*	*Ovol1*	*Pitx2*	*Ppard*
Sp5	*Tbx1*	*Tbx3*	*Tcf4*	*Tcf7*	*Tert*	*Tnfrsf19*	*Vcan*
Vegfa							

Table S11: The applied statistical methods and results for each figure.

Figure #	Group	n	Shapiro-Wilk normality test P value (if applied)	Applied statistical test(s) and result(s)
1B-CHO	WT	11	0.8443	Unpaired Student`s *t*-test, two-tailed, P=0.0001
	KO	8	0.2657	
1B-TG	WT	11	0.7305	Unpaired Student`s *t*-test, two-tailed, P=0.0002
	KO	8	0.4070	
1B-HDL	WT	11	0.0275	Mann-Whitney *U*-test, two-tailed, P=0.3403
	KO	8	0.2529	
1B-LDL	WT	11	0.9707	Mann-Whitney *U*-test, two-tailed, P=0.0012
	KO	8	0.0051	
1C	WT	11	0.7647	Unpaired Student`s *t*-test, two-tailed, P=0.4258
	KO	8	0.7468	
1D	WT	11	0.5482	Unpaired Student`s *t*-test, two-tailed, P=0.0129
	KO	8	0.0846	
1E	WT	11	0.0082	Mann-Whitney *U*-test, two-tailed, P=0.7168
	KO	8	0.3586	
1F	WT	11	0.1367	Mann-Whitney *U*-test, two-tailed, P=0.5448
	KO	8	0.0165	
1G-% lesion	WT	11	0.0006	Mann-Whitney *U*-test, two-tailed, P=0.0409
	KO	8	0.1952	
1G-Absolute	WT	11	0.0012	Mann-Whitney *U*-test, two-tailed, P=0.0259
	KO	8	0.2951	
1H	WT	11	0.1817	Unpaired Student`s *t*-test, two-tailed, P=0.0135
	KO	10	0.3026	
2H	WT	6	0.1387	Unpaired Student`s *t*-test, two-tailed, P=0.0008
	KO	6	0.5391	
2I	WT	6	0.5691	Unpaired Student`s *t*-test, two-tailed, P=0.0355
	KO	6	0.0842	
2J-ACAN	WT	6	0.5829	Unpaired Student`s *t*-test, two-tailed, P=0.0154
	KO	6	0.6674	
2J-CHAD	WT	6	0.0002	

	KO	6	0.0049	Mann-Whitney *U*-test, two-tailed, P=0.0087
3C-CHO	BM WT	8	0.3195	Unpaired Student`s *t*-test, two-tailed, P=0.5881
	BM KO	8	0.0628	
3C-TG	BM WT	8	0.1523	Unpaired Student`s *t*-test, two-tailed, P=0.8143
	BM KO	8	0.1553	
3C-HDL	BM WT	8	0.2698	Unpaired Student`s *t*-test, two-tailed, P=0.3357
	BM KO	8	0.6045	
3C-LDL	BM WT	8	0.2826	Unpaired Student`s *t*-test, two-tailed, P=0.0823
	BM KO	8	0.1120	
3D	BM WT	8	0.2864	Mann-Whitney *U*-test, two-tailed, P=0.5737
	BM KO	8	0.0277	
3E	BM WT	8	0.7140	Unpaired Student`s *t*-test, two-tailed, P=0.6109
	BM KO	8	0.7934	
3F	BM WT	8	0.5616	Unpaired Student`s *t*-test, two-tailed, P=0.2398
	BM KO	8	0.5054	
3G-% lesion	BM WT	8	0.0000	Mann-Whitney *U*-test, two-tailed, P>0.9999
	BM KO	8	0.0007	
3G-Absolute	BM WT	8	0.0001	Mann-Whitney *U*-test, two-tailed, P>0.9999
	BM KO	8	0.0001	
3H	BM WT	8	0.4348	Unpaired Student`s *t*-test, two-tailed, P=0.4878
	BM KO	8	0.1895	
3I	BM WT	8	0.1629	Unpaired Student`s *t*-test, two-tailed, P=0.6746
	BM KO	8	0.8220	
5G-Ibsp & Acan	WT	5	-	Mann-Whitney *U*-test, two-tailed, P=0.0159
	KO	4	-	
5G-Ibsp	WT	5	-	Mann-Whitney *U*-test, two-tailed, P=0.0159
	KO	4	-	
5G-Acan	WT	5	-	Mann-Whitney *U*-test, two-tailed, P=0.0635
	KO	4	-	
6B-Aortic media	SMC WT	4	-	Mann-Whitney *U*-test, two-tailed, P=0.0286
	SMC KO	4	-	
6B-Adventitia	SMC WT	4	-	Mann-Whitney *U*-test, two-tailed, P=0.0286
	SMC KO	4	-	
6B-Liver	SMC WT	4	-	Mann-Whitney *U*-test, two-tailed, P=0.8857
	SMC KO	4	-	
6B-Quadriceps m.	SMC WT	4	-	Mann-Whitney *U*-test, two-tailed, P=0.8857
	SMC KO	4	-	
6D-CHO	SMC WT	12	0.2476	Mann-Whitney *U*-test, two-tailed, P=0.8667
	SMC KO	15	0.0274	
6D-TG	SMC WT	12	0.0244	Mann-Whitney *U*-test, two-tailed, P=0.7551
	SMC KO	15	0.5968	
6D-HDL	SMC WT	12	0.7902	Unpaired Student`s *t*-test, two-tailed, P=0.1918
	SMC KO	15	0.1796	

6D-LDL	SMC WT	12	0.2553	Unpaired Student`s *t*-test, two-tailed, P=0.5385
	SMC KO	15	0.3810	
6E	SMC WT	12	0.9960	Unpaired Student`s *t*-test, two-tailed, P=0.5950
	SMC KO	15	0.6536	
6F	SMC WT	12	0.2134	Unpaired Student`s *t*-test, two-tailed, P=0.2635
	SMC KO	15	0.0541	
6G	SMC WT	12	0.4125	Unpaired Student`s *t*-test, two-tailed, P=0.8936
	SMC KO	15	0.1057	
6H-% lesion	SMC WT	12	0.0010	Mann-Whitney *U*-test, two-tailed, P=0.0289
	SMC KO	15	0.0006	
6H-Absolute	SMC WT	12	0.0001	Mann-Whitney *U*-test, two-tailed, P=0.0542
	SMC KO	15	0.0002	
6I	SMC WT	12	0.2185	Unpaired Student`s *t*-test, two-tailed, P=0.0438
	SMC KO	15	0.2115	
6J	SMC WT	12	0.0437	Mann-Whitney *U*-test, two-tailed, P=0.0924
	SMC KO	15	0.1561	
7B-Ly6a	P0	4	-	One-way ANOVA: P=0.0008 Dunnett`s multiple comparisons: (1) P0 vs. P1, P=0.0012 (2) P0 vs. P2, P=0.0012
	P1	4	-	
	P2	4	-	
7B-Lum	P0	4	-	One-way ANOVA: P=7.00E-06 Dunnett`s multiple comparisons: (1) P0 vs. P1, P=0.0001 (2) P0 vs. P2, P=0.0104
	P1	4	-	
	P2	4	-	
7B-Myh11	P0	4	-	One-way ANOVA: P=1.13E-06 Dunnett`s multiple comparisons: (1) P0 vs. P1, P=0.0001 (2) P0 vs. P2, P=0.0001
	P1	4	-	
	P2	4	-	
7C	NC	4	-	Unpaired Student`s *t*-test, two-tailed, P=3.53E-07
	si-Txnip	4	-	
7D	NC	5	-	Unpaired Student`s *t*-test, two-tailed, P=0.0007
	si-Txnip	5	-	
7E-Sp7	OD- NC	4	-	One-way ANOVA: P=3.19E-05 Holm-Sidak`s multiple comparisons: (1) OD- NC vs. OD- si-Txnip, P= 0.8656 (2) OD+ NC vs. OD+ si-Txnip, P=4.08E-05
	OD- si-Txnip	4	-	
	OD+ NC	4	-	
	OD+ si-Txnip	4	-	
7E-Bglap	OD- NC	4	-	One-way ANOVA: P=4.78E-10 Sidak`s multiple comparisons: (1) OD- NC vs. OD- si-Txnip, P=0.9980 (2) OD+ NC vs. OD+ si-Txnip, P=7.81E-10
	OD- si-Txnip	4	-	
	OD+ NC	4	-	
	OD+ si-Txnip	4	-	
7E-Ibsp	OD- NC	4	-	One-way ANOVA: P=2.50E-07 Sidak`s multiple comparisons: (1) OD- NC vs. OD- si-Txnip, P=4.77E-07 (2) OD+ NC vs. OD+ si-Txnip, P=3.21E-05
	OD- si-Txnip	4	-	
	OD+ NC	4	-	
	OD+ si-Txnip	4	-	
7E-Myh11	OD- NC	4	-	One-way ANOVA: P=0.0017 Sidak`s multiple comparisons:
	OD- si-Txnip	4	-	

	OD+ NC	4	-	(1) OD- NC vs. OD- si-Txnip, P=0.1337
	OD+ si-Txnip	4	-	(2) OD+ NC vs. OD+ si-Txnip, P=0.0497
7G-Bmp2	OD- NC	4	-	One-way ANOVA: P=0.0207 Sidak`s multiple comparisons: (1) OD- NC vs. OD+ NC, P=0.0476 (2) OD+ NC vs. OD+ si-Txnip, P=0.6841
	OD- si-Txnip	4	-	
	OD+ NC	4	-	
	OD+ si-Txnip	4	-	
7G-Bmp4	OD- NC	4	-	One-way ANOVA: P=0.0014 Sidak`s multiple comparisons: (1) OD- NC vs. OD+ NC, P=0.0043 (2) OD+ NC vs. OD+ si-Txnip, P=0.8020
	OD- si-Txnip	4	-	
	OD+ NC	4	-	
	OD+ si-Txnip	4	-	
7H-Id1	OD- NC	4	-	One-way ANOVA: P=0.0255 Sidak`s multiple comparisons: (1) OD- NC vs. OD- si-Txnip, P=0.3888 (2) OD+ NC vs. OD+ si-Txnip, P=0.0127
	OD- si-Txnip	4	-	
	OD+ NC	4	-	
	OD+ si-Txnip	4	-	
7H-Id2	OD- NC	4	-	One-way ANOVA: P=3.90E-05 Sidak`s multiple comparisons: (1) OD- NC vs. OD- si-Txnip, P=0.9184 (2) OD+ NC vs. OD+ si-Txnip, P=4.19E-05
	OD- si-Txnip	4	-	
	OD+ NC	4	-	
	OD+ si-Txnip	4	-	
7H-Id3	OD- NC	4	-	One-way ANOVA: P=0.0049 Sidak`s multiple comparisons: (1) OD- NC vs. OD- si-Txnip, P=0.0421 (2) OD+ NC vs. OD+ si-Txnip, P=0.0407
	OD- si-Txnip	4	-	
	OD+ NC	4	-	
	OD+ si-Txnip	4	-	
7H-Id4	OD- NC	4	-	One-way ANOVA: P=6.92E-08 Sidak`s multiple comparisons: (1) OD- NC vs. OD- si-Txnip, P=0.2401 (2) OD+ NC vs. OD+ si-Txnip, P=6.08E-08
	OD- si-Txnip	4	-	
	OD+ NC	4	-	
	OD+ si-Txnip	4	-	
8B-Cyto	NC	4	-	Unpaired Student`s *t*-test, two-tailed, P=0.0002
	si-Txnip	4	-	
8B-Nuclear	NC	4	-	Unpaired Student`s *t*-test, two-tailed, P=0.0027
	si-Txnip	4	-	
8F	K02288- NC	4	-	One-way ANOVA: P=1.09E-10 Sidak`s multiple comparisons: (1) K02288- NC vs. K02288- si-Txnip, P=3.70E-10 (2) K02288+ NC vs. K02288+ si-Txnip, P=0.9998 (3) K02288- si-Txnip vs. K02288+ si-Txnip, P=2.47E-10
	K02288- si-Txnip	4	-	
	K02288+ NC	4	-	
	K02288+ si-Txnip	4	-	
8G-si-Smad4	NC	4	-	Unpaired Student`s *t*-test, two-tailed, P=2.85E-05
	si-Smad4	4	-	
8G-si-MAPK14	NC	4	-	Unpaired Student`s *t*-test, two-tailed, P=0.0007
	si-MAPK14	4	-	

8I	si-Txnip-/si-Smad4-/si-MAPK14-	4	-	One-way ANOVA: P=2E-15 Holm-Sidak`s multiple comparison: (1) si-Txnip-/si-Smad4-/si-MAPK14- vs. si-Txnip+/si-Smad4-/si-MAPK14-, P=1.88E-13 (2) si-Txnip-/si-Smad4-/si-MAPK14- vs. si-Txnip+/si-Smad4+/si-MAPK14-, P=0.5608 (3) si-Txnip-/si-Smad4-/si-MAPK14- vs. si-Txnip+/si-Smad4-/si-MAPK14+, P=0.1138 (4) si-Txnip-/si-Smad4-/si-MAPK14- vs. si-Txnip+/si-Smad4+/si-MAPK14+, P=0.4045
	si-Txnip+/si-Smad4-/si-MAPK14-	4	-	
	si-Txnip-/si-Smad4+/si-MAPK14-	4	-	
	si-Txnip+/si-Smad4+/si-MAPK14-	4	-	
	si-Txnip-/si-Smad4-/si-MAPK14+	4	-	
	si-Txnip+/si-Smad4-/si-MAPK14+	4	-	
	si-Txnip-/si-Smad4+/si-MAPK14+	4	-	
	si-Txnip+/si-Smad4+/si-MAPK14+	4	-	
S1-En face	WT	6	-	Mann-Whitney *U*-test, two-tailed, P=0.0303
	KO	5	-	
S1-Lower thoracic	WT	6	-	Mann-Whitney *U*-test, two-tailed, P=0.0455
	KO	5	-	
S1-Abdominal	WT	6	-	Mann-Whitney *U*-test, two-tailed, P=0.0390
	KO	5	-	
S1B	WT	5	-	Mann-Whitney *U*-test, two-tailed, P=0.0357
	KO	3	-	
S1C	WT	5	-	Mann-Whitney *U*-test, two-tailed, P=0.0357
	KO	3	-	
S5B	WT	5	-	Mann-Whitney *U*-test, two-tailed, P=0.7302
	KO	4	-	
S10	Non-cal	4	-	Mann-Whitney *U*-test, two-tailed, P=0.0571
	Cal		-	
S11	SMC WT	4	-	Unpaired Student`s *t*-test, two-tailed, P=0.0007
	SMC KO	4	-	
S12A-Smad1	NC	4	-	Unpaired Student`s *t*-test, two-tailed, P=0.0648
	si-Txnip	4	-	
S12A-Smad5	NC	4	-	Unpaired Student`s *t*-test, two-tailed, P=0.0343
	si-Txnip	4	-	
S12A-Smad4	NC	4	-	Unpaired Student`s *t*-test, two-tailed, P=0.0093
	si-Txnip	4	-	

S12A-Smad7	NC	4	-	Unpaired Student`s *t*-test, two-tailed, P=0.0620
	si-Txnip	4	-	
S12B-Smad1	MG132- NC	4	-	One-way ANOVA: P=1.34E-05 Holm-Sidak`s multiple comparisons: (1) MG132- NC vs. MG132- si-Txnip, P=0.0062 (2) MG132+ NC vs. MG132+ si-Txnip, P=0.6928
	MG132- si-Txnip	4	-	
	MG132+ NC	4	-	
	MG132+ si-Txnip	4	-	
S12B-Smad5	MG132- NC	4	-	One-way ANOVA: P=0.0310 Holm-Sidak`s multiple comparisons: (1) MG132- NC vs. MG132- si-Txnip, P=0.0390 (2) MG132+ NC vs. MG132+ si-Txnip, P=0.8100
	MG132- si-Txnip	4	-	
	MG132+ NC	4	-	
	MG132+ si-Txnip	4	-	
S12B-Smad7	MG132- NC	4	-	One-way ANOVA: P=4.31E-06 Holm-Sidak`s multiple comparisons: (1) MG132- NC vs. MG132- si-Txnip, P=0.0030 (2) MG132+ NC vs. MG132+ si-Txnip, P=6.25E-05
	MG132- si-Txnip	4	-	
	MG132+ NC	4	-	
	MG132+ si-Txnip	4	-	
S12C-BMPR1A	NC	4	-	Unpaired Student`s *t*-test, two-tailed, P=0.3521
	si-Txnip	4	-	
S12C-Smurf1	NC	4	-	Unpaired Student`s *t*-test, two-tailed, P=0.1997
	si-Txnip	4	-	
S12C-Smurf2	NC	4	-	Unpaired Student`s *t*-test, two-tailed, P=0.4957
	si-Txnip	4	-	
S12F	NC	4	-	Unpaired Student`s *t*-test, two-tailed, P=0.6978
	si-Txnip	4	-	

1

Supplemental Discussion

Significance and limitations of *in vivo* mouse models used in our study

In the *in vivo* experiment, we utilized three different mouse models (TXNIP ablation in the whole genome, hematopoietic cells, and SMCs) to analyze the effect of TXNIP on atherosclerotic calcification through a complementary interpretation of the results. Although VSMCs are considered to be the major cell type that contribute atherosclerotic calcification, other cell types, such as macrophages,[30] endothelial cells,[59] and adventitial cells,[60] can also contribute to atherosclerotic calcification, and the interactions between these various cells can also shape atherosclerotic phenotypes. Therefore, we initially attempted to characterize the effect of TXNIP on advanced atherosclerotic lesions in combination with scRNA-seq analysis using *Txnip* KO (*Txnip*$^{-/-}$) mice. Of note, Byon et al. previously showed a reduced atherosclerotic burden in *Txnip*$^{-/-}$; *ApoE*$^{-/-}$ mice under chow diet condition.[20] However, the atherosclerotic lesions observed in this study were not considered sufficient for interrogating the advanced lesion phenotypes, probably due to absence of HFD feeding. By conducting BMT experiments, we ruled out the possible effects of immune cells on atherosclerotic calcification, such as macrophage-produced matrix vesicles, nucleating sites, or calcification-facilitating microenvironments.[7, 30] Lastly, we utilized *Tagln*-Cre; *Txnip*$^{flox/flox}$ mice to specifically investigate the role of TXNIP on VSMCs. Of note, *Tagln* can be also partially or transiently expressed in other cells such as myofibroblasts, and perivascular adipose cells, as well as in their precursors.[36] In addition, other cell types such as endothelial cells (via endothelial-to-mesenchymal transition)[61, 62] or adventitial progenitor cells[63, 64] can gain *Tagln* expression and contribute to atherosclerotic calcification.[59, 60] Therfore, it appears that increased calcification in our *Tagln*-Cre; *Txnip*$^{flox/flox}$ mice can not be solely attributable to VSMCs, suggesting a limitation of the model. We partially complement this limitation by demonstrating augmented osteodifferentiation in primary cultured VSMCs upon TXNIP suppression. Additional *in vivo* studies employing inducible Cre (e.g., Cre^{ERT2}) could further refine our results.

Characterization of the osteogenic and chondrogenic populations in mice atheroma

In this study, we attempted to further characterize the osteochondrogenic cluster of atherosclerotic lesions in mice into osteogenic and chondrogenic populations. We found that *Ibsp*$^{+}$*Acan*$^{-}$ cells were enriched in the proximity of the calcified area, suggesting that atherosclerotic calcification may indeed mimic the normal bone mineralization process by osteogenic cells. In the cartilage metaplasia area, *Ibsp*$^{-}$*Acan*$^{+}$ cells were mainly observed but

there were also some *Ibsp*$^{+}$*Acan*$^{-}$ cells, and the ablation of TXNIP increased the proportion of *Ibsp*$^{+}$*Acan*$^{-}$ cells. Since there were mixed areas of calcification and cartilage metaplasia, we speculated that *Ibsp*$^{+}$*Acan*$^{-}$ cells of the cartilage metaplasia area may represent cells undergoing endochondral ossification in the atherosclerotic lesion, as previously suggested,[34] and that this process might be enhanced in *Txnip* KO mice. Otherwise, the *Ibsp*$^{+}$*Acan*$^{-}$ cells themselves may indicate dysregulated osteochondrogenic processes in the atherosclerotic lesions. Meanwhile, the osteochondrogenic cluster in the scRNA-seq data did not clearly separated into osteogenic and chondrogenic populations (i.e., expressing both osteogenic and chondrogenic markers), showing the extent of some of the discrepancies between the *in situ* hybridization data. ScRNA-seq has several technical elements that have to be considered, such as a relatively shallow sequencing depth, which can cause bias toward highly expressed genes, or the underestimation of hard-to-isolate cells.[46] Particularly in the latter case, terminally differentiated osteocytes and/or chondrocytes in atherosclerotic lesions may not be properly captured in the scRNA-seq data. Further studies will be required to accurately characterize the osteogenic and chondrogenic cells and their differentiation process in atherosclerotic lesions.

Possible roles of TXNIP in other cell types and cardiovascular diseases

The other remaining questions are as follows. (1) Does the regulatory role of TXNIP in BMP signaling also works in other cell types? BMP signaling not only plays a central role in bone morphogenesis, but is also involved in various physiological and embryogenic processes.[65] As we did not observe any notable skeletal or developmental anomalies in *Txnip* KO mice, the regulatory effect of TXNIP on BMP signaling is not likely pan-cellular. However, these possibilities still remain. (2) What is the role of TXNIP in other cardiovascular diseases that involve the phenotypic modulation of VSMCs (e.g., medial artery calcification, hypertension, pulmonary arterial hypertension, cerebral microangiopathy, Marfan syndrome?[66] Further studies are required to address these questions.